Electronic Supplementary Material (ESI) for RSC Advances.
This journal is © The Royal Society of Chemistry 2020

Supporting Information

Essential Oil Loaded Pectin/Chitosan Nanoparticles Preparation and optimization via Box–Behnken Design against MCF-7 Breast Cancer Cell Lines

Olivia A. Attallah[a,b], Amro Shetta[a], Fatma Elshishiny[a] and Wael Mamdouh[*a]

[a]*Department of Chemistry, School of Sciences and Engineering (SSE), The American University in Cairo (AUC), AUC Avenue, P.O. Box 74, New Cairo 11835, Egypt.*

[b]*Pharmaceutical Chemistry Department, Faculty of Pharmacy, Heliopolis University, Cairo - Belbeis Desert Road, El Salam, Cairo 11777, Egypt*

1. Experimental

1.1. Materials

Pec from the rind of citrus or apple (Galacturonic acid ≥74.0%) was obtained from Fisher Scientific (USA). CS of low molecular weight (89.9% degree of dealkylation) was purchased from (Primex ehf, Chitoclear, Iceland), Calcium chloride dihydrate, 2,2-diphenyl-1-picrylhydrazyl radical (DPPH), and Dichloromethane were obtained from Sigma Aldrich Co. (USA). JO was purchased from Nefertari Natural Body Care Line (Cairo, Egypt). Dulbecco's modified Eagle's medium (DMEM), Fetal bovine serum (FBS), Trypsin EDTA, Penicillin/Streptomycin, Phosphate buffer solution (PBS) was obtained from Lonza, Switzerland. MTT reagent, 3-[4,5-dimethyl-2-thiazolyl]-2,5-diphenyl-2H-tetrazolium bromide and dimethyl sulfoxide (DMSO), was purchased from Serva Electrophoresis, Heidelberg, Germany. All other chemicals and reagents used were of analytical grade.

1.2. Instrumentation

The morphologies and elemental composition of the synthesized NPs were characterized using transmission electron microscopy (TEM) on Tecani G20, FEI transmission electron microscope (USA) and scanning electron microscopy coupled with energy dispersion x-ray technique (SEM/EDX) in a Zeiss instrument (Germany), respectively. The crystalline structure of the synthesized NPs was characterized by X-ray diffractometer (a Bruker AXS D8, Germany) over a 2θ range from 10 to 70◦ (2θ) at a scan rate of 4◦min-1. Fourier transform infrared (FT-IR) spectra (KBr pellets) over the range of 400–4000 cm−1 were performed on a Thermo Scientific Nicolet 8700 spectrophotometer, USA. The thermal degradation and crystallization process of the prepared NPs were investigated using a Q50 Thermogravimetric Analyzers, TA, USA. The measurement was conducted under N2 atmosphere from 20 to 600°C at a

heating rate of 10°C/min. The concentrations of JO in the solutions were detected by a UV-Vis model AE-S90-MD form A & E Lab (UK).

1.3. Design of experiment

Three-factor, three-level Box-Behnken design (Design Expert, trial version 10.0.5.0, Stat-Ease Inc., Minneapolis, MN) was implemented for optimization of Pec/CS/JO (Pec/CS/JO) NPs. This design involved 15 experimental runs with three replicated center points. The independent factors were Pec concentration (X_1), CS concentration (X_2), and $CaCl_2$ concentration (X_3). The three variables were varied at three levels: low (coded as -1), middle (coded as 0) and high (coded as 1). The concentration of JO was kept constant at 5.0 mg. The fabrication process being very simple, no process parameters were assumed to exert significant effect on the responses and were not selected for BBD studies. The responses or dependent variables studied were particle size (Y1), ZP (Y2), EE% (Y3) and poly dispersity index (PDI) (Y4). The ranges (low and high level) for each independent factor were selected based on published reports [1–5] and preliminary experiments performed to obtain a good colloidal suspension of NPs. Selected ranges are shown in (Table S1).

Table S1: Variables and constrains in Box-Behnken experimental design

	level			
Independent variables	-1	0	1	Constrains
X_1: Pectin Conc. (wt%)	0.03	0.05	0.07	In the range
X_2: Chitosan Conc. (wt%)	0.015	0.025	0.035	In the range
X_3: $CaCl_2$ Conc. (wt%)	0.006	0.009	0.012	In the range
Dependent variables				
Y_1: Particle size (nm)				Minimize
Y_2: Zeta Potential (mV)				-20 to -27
Y_3: Encapsulation Efficiency (%)				Maximize
Y_4: PDI				-

1.4. Optimization of Pec/CS/JO NPs by multiple responses

In this study, all three responses were simultaneously optimized by using BBD optimization [6]. The optimum formulation was selected based on the criteria of attaining the minimum particle size, maximum EE% and applying constrains on ZP (-20 to -27).

1.5. Preparation of Pec/CS/JO NPs

Briefly, Pec solution (1 gm%) was prepared by dissolving Pec powder in distilled water (DW) containing 0.05M NaCl using a magnetic stirrer (300 rpm for 24 hrs) at room temperature (25 °C). To 60 mL Pec solution, different JO solutions (0, 2.5, 5.0, 7.5, and 10.0 mg JO that were previously dissolved in DCM) were mixed forming emulsion dispersion. Pec/CS/JO NPs were then prepared by inotropic gelation at room temperature using CS/$CaCl_2$ mixture [4]. CS solution (1% (w/v)) was prepared by mixing CS powder with 1% acetic acid (w/v), then stirred overnight, while $CaCl_2$ solution (0.25% (w/v)) was prepared by dissolving $CaCl_2$ in DW. 15mL of CS-$CaCl_2$ mixture solutions prepared in 0.05M NaCl were added dropwise to the 60 mL Pec/JO emulsion under 550 rpm stirring for 30 min. Formulations were prepared by mixing various proportions of Pec, CS and $CaCl_2$ as suggested by the BBD matrix. All other preparation parameters were kept constant and JO was stabilized at 5.0 mg concentration. The prepared NPs were centrifuged at 10000 rpm for 15 min, followed by washing several times by distilled water. Finally, the collected wet pellets were dispersed in DW and freeze dried at (-65 °C) for 72 hrs. The NPs were stored in a desiccator until further analysis.

1.6. Spectrophotometric analysis of JO

Stock solution of JO (0.1mg/mL) was prepared in 100 mL volumetric flask using dichloromethane (DCM). Solutions were scanned in the range of 200–400 nm and the wavelength of maximum absorption for JO was determined. Accurate volumes of JO stock solutions were transferred into 25 mL volumetric flasks separately and diluted to volume with DCM. Calibration curve for the investigated oil was obtained by plotting absorbance at λmax=285 nm against concentration. Various assay validation parameters were then calculated according to ICH guidelines [7–9].

1.7. Determination of particle size, PDI and ZP

The particle size, PDI and ZP of freshly prepared NPs were analyzed by a Malvern nano-series Zetasizer with non-invasive back scatter technology, which analyses at a wavelength of 633 nm, scattering angle of 90° at 25°C and detects dispersion of light caused by the Brownian motion of droplets. The Z-average diameter, also called the hydrodynamic droplet diameter, was measured with three different batches. The measurements of droplet size, PDI and ZP of optimized Pec/CS/JO NPs were carried out in the same way.

1.8. Determination of encapsulation efficiency (EE%) and Loading Capacity (LC%)

Predetermined amounts of Pec/CS/JO NPs were dispersed into 25mL 0.01N HCl in ethanol and magnetically stirred for 1 h at 550 rpm then centrifuged at 10000 rpm for 20 min at (25 °C). The supernatant was analyzed for the JO content using UV–Vis

spectrophotometry at a wavelength of 285nm. EE% and LC% were estimated from equations (1) and (2) respectively [10].

$$EE\ (\%) = \frac{Total\ amount\ of\ loaded\ JO}{Initial\ amount\ of\ JO} \times 100 \quad (1)$$

$$LC\ (\%) = \frac{Total\ amount\ of\ loaded\ JO}{Weight\ of\ NPs\ after\ freeze\ drying} \times 100 \quad (2)$$

1.9. *In-vitro* release studies

The *in-vitro* release study of JO from Pec/CS NPs was carried out in different pH media; phosphate buffer saline (PBS) with a pH of 7.4 and acetate buffer with a pH of 3.0 and 5.5, respectively. To study the in-vitro release, 25 mg of lyophilized Pec/CS/JO NPs was placed in a dialysis bag (12000–14,000 KDa), containing 5 mL of release media (PBS or acetate buffer) and incubated in 25 mL of the same release media under gentle shaking. A specific volume of release media at predetermined sampling time intervals was withdrawn for analysis, with the addition of an equal volume of fresh release media. The total cumulative amount of JO (mg) in the release medium (mL) was estimated through UV–Vis spectrophotometer at wavelength of 285nm. The loading capacity (LC%) of JO in JO/Pec/CS NPs was determined to help in the calculation of initial amount of JO encapsulated in the NPs (M_0). The percentage of cumulative JO released was then presented by the ratio of the cumulative amount of JO released at each time interval (M_t) to the initial amount of the JO encapsulated in the NPs (M_0) as illustrated in Eq. (1) [11]. To study the kinetic profile of JO release from Pec/CS/JO NPs, data was treated according to zero-order, first-order, Higuchi, Korsmeyer- Peppas, and Hixson-Crowell equations [12–14].

$$Cumulative\ release\ percentage \sum_{t=0}^{t} \frac{M_t}{M_0} x\ 100 \quad (1)$$

1.10. Stability of total phenolic contents of JO in Pec/CS NPs

Total phenolic contents (TPC) of pure JO and Pec/CS/JO NPs were estimated using Folin–Ciocalteu method as reported by Esmaeili *et al.* with slight modifications [15]. Briefly, pure JO (10 mg), Pec/CS NPs (15 mg) and Pec/CS/JO NPs (15 mg) were mixed separately with 2 mL ethanol then 2.5 mL of (10% v/v) aqueous Folin–Ciocalteu reagent was added and left for 4 min. 2 mL aqueous solution of (7.5% w/v) sodium carbonate was then dropped to the mixture and left in the dark for 48 hrs at room temperature. Finally, samples were centrifuged at 10000 rpm for 3 min and the supernatant was removed for

measuring the absorbance at 765 nm using UV-Vis spectrophotometer. To estimate the TPC, different concentrations of Gallic acid (0.01–0.1 mg/mL) in ethanol were treated like the samples to develop a gallic acid standard calibration curve (R2 of 0.99). The gallic acid equivalent (GAE) which expresses the amount of gallic acid in mg that is equivalent to 1 g of JO was calculated using the regression equation of the calibration curve.

1.11. Determination of the Antioxidant Activity

The antioxidant activity of Pec/CS/JO NPs were examined using DPPH free radical scavenging assay as illustrated by Shetta et al. [22] with slight modification. 2mL of predetermined amounts of pure JO, Pec/CS NPs and Pec/CS/JO NPs dissolved in ethanol were added to 2mL of (ethanol DPPH solution (0.1mM)) and stored in the dark for 2 hours at room temperature. The samples containing NPs were centrifuged for 3 min to take the supernatant for analysis. Spectrophotometer at a wavelength of 517 nm was used to measure the absorbance of samples and dehydrated ethanol was used as a blank. Gallic acid was considered a reference standard and DPPH solution was used as the control. The DPPH radical-scavenging activity (%) was calculated using Eq. (2) [11]. The IC50 (the sample concentration providing 50% of radicals scavenging activity) value was calculated from the graph by linear regression analysis [11].

$$DPPH\ scavenging\ activity\ (\%) = \frac{A_{control} - A_{sample}}{A_{control}} \times 100 \quad (2)$$

Where $A_{control}$ is the DPPH absorbance and A_{sample} is the sample absorbance.

1.12. Cytotoxicity studies

1.12.1. Cell line maintenance

A human breast cancer cell line (MCF-7) and a normal mouse fibroblast cell line (L-929) were used as an *in-vitro* model to evaluate the activity of bare Pec/CS NPs, Pure JO and encapsulated JO in Pec/CS NPs, independently. Both cell lines were cultured separately as a monolayer in DMEM supplemented with 4500 mg/L glucose, L-glutamine, sodium pyruvate, sodium bicarbonate, 10% FBS, and 5% penicillin/streptomycin. The cells were passaged in 75 cm2 tissue culture flasks and incubated in 5% CO_2 incubator (Heracell incubator, Thermo Scientific, USA) at 37°C. Trypsin (0.25%) containing 0.1% EDTA was used in cell detachment before passaging interval times. Trypan blue was used in cell counting using hemocytometer.,bare Pec/CS NPs, Pure JO and Pec/CS/JO NPs samples were sterilized for 1 h using UV radiation.

1.12.2. Direct Cytotoxicity (MTT assay)

The anticancer activity of JO before and after encapsulation in Pec/CS NPs against MCF-7 cells and their cyto-compatibility against L-929 cells were investigated according to the ISO10993-5 standard based procedure. MCF-7

and L-929 cells were seeded separately in 96 well plate to reach semi-confluent growth after 24 hrs. Following that, 100µL of previously prepared serial dilutions of bare Pec/CS (0.5 – 10.0 mg/mL), pure JO (0.3 – 3 mg/mL) and encapsulated JO in Pec/CS NPs (0.03 – 0.6 mg/mL) and were directly added to the overnight seeded cells. After 24 hrs, the media/treatment solutions were replaced by 100 uL of 1 mg/mL MTT reagent for each well and incubated for 4 hrs in 5% CO_2. Then, the cells were washed with PBS twice after removing the MTT medium and 100 uL/well of 100% DMSO was added to dissolve the formazan crystals formed in living cells. Cell viability was identified using microplate reader (SPECTROstar Nano, BMG LABTECH, Germany) at absorbance of 570 nm. The viability of control cells was recognized as 100% and calculated according to Eq. (3):

$$\text{Percent of Cell Viability}(\%)=(\text{Sample Abs})/(\text{Control Abs})\times 100 \quad (3)$$

Where the Abs stands for the sample absorbance at 570 nm.

The IC_{50} for anticancer activity was extrapolated from the dose-response graph. The concentrations of pure JO, bare Pec/CS NPs and encapsulated JO in Pec/CS NPs that reduced the viability of cells by 50% (IC_{50}) were determined by plotting data points over the specified concentration ranges and calculating values using regression equation.

1.13. Statistical analysis

Results are reported as the mean ± SD for triplicate measurements. Statistical analysis of the data was carried out via one-way ANOVA followed by Tukey's test to compare the treatment means using GraphPad prism software (version 5 trial version). Statistical significance was expressed at $P < 0.05$.

2. Supplementary results, figures and tables

S1 Mechanism of crosslinking

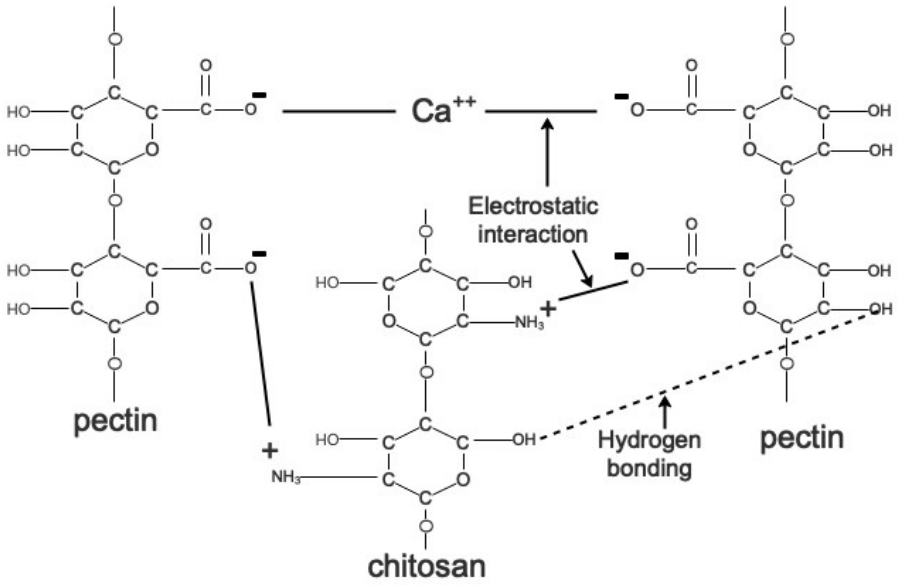

Fig. S1: Pec/CS/Ca^{+2} ion cross-linking mechanisms

S2 Spectrophotometric analysis of JO

The wavelength of maximum absorption (λmax) was determined for JO and was found to be 285 nm. The method was validated according to ICH Q2B guidelines for validation of analytical procedures as regards in linearity, accuracy, precision (within and between days), limit of detection (LOD), and limit of quantification (LOQ) [7–9]. The validation results are summarized in Table S1. Results indicated the suitability of the assay for accurate determination of the studied oil in neat solvent for optimization purposes.

Table S2: Spectrophotometric method validation for the determination of laboratory prepared standards of Jasmine Oil (JO)

Item	**JO**
Wavelength of detection	285 nm
Range of linearity	2-24 µg.mL^{-1}
Regression equation	A=0.0405C +0.037
Regression coefficient (r)	0.9998
LOD (µg.mL^{-1})	0.48
LOQ (µg.mL^{-1})	1.45

Accuracy	99.41 ± 1.31
Mean ± SD	
Precision	
Intraday %RSD (n = 9)	1.355
Interday %RSD (n = 9)	1.588

S3 BDD

Table S3: Experimental matrix and observed responses from randomized runs in BBD

	Independent variable			**Dependent variable**			
Run	X_1 (wt%)	X_2 (wt%)	X_3 (wt%)	Y_1 (nm)	Y_2 (mV)	Y_3 (%)	PDI
1	-1	0	+1	552.7	-18.1	24.98	0.18
2	+1	+1	0	676.6	-25.4	28.01	0.369
3	+1	0	+1	698.3	-24.5	27.56	0.306
4	0	0	0	575.9	-22.4	25.46	0.369
5	0	-1	-1	547.2	-23.5	24.57	0.286
6	-1	0	-1	525.5	-18.6	24.92	0.449
7	0	0	0	579	-21.9	25.18	0.323
8	-1	-1	0	468.5	-20.8	24.41	0.4
9	0	0	0	570	-23	25.47	0.33
10	0	+1	+1	620.3	-20.8	26.12	0.393
11	+1	0	-1	650.3	-25.4	26.67	0.309
12	0	-1	+1	569.4	-22.8	24.57	0.351
13	0	+1	-1	586.4	-21.5	25.89	0.117
14	-1	+1	0	548.3	-19.5	25.49	0.457
15	+1	-1	0	625.2	-27.1	26.16	0.296

Table S4: Statistical analysis of measured responses

Fitting model	Factors	Coefficient	P-value	ANOVA
Particle size (Y_1)	Intercept	574.97		F = 84.61,
	X_1	69.42	*< 0.0001*	R^2 = 0.9935,
	X_2	27.66	*0.0002*	Model P-value
	X_3	16.41	*0.0022*	<0.0001,
	X_1X_2	-7.10	*0.1386*	P-value of lack
	X_1X_3	5.20	*0.2536*	of fit = 0.1865
	X_2X_3	2.93	*0.5007*	
	X_1^2	15.28	*0.0149*	
	X_2^2	-10.60	*0.0529*	
	X_3^2	16.45	*0.0112*	
Zeta Potential (Y_2)	Intercept	-22.43		F = 60.22,
	X_1	-3.17	*< 0.0001*	R^2 = 0.9909,
	X_2	0.88	*0.0019*	Model P-value
	X_3	0.35	*0.0623*	= 0.0001,
	X_1X_2	0.100	*0.6494*	P-value of lack
	X_1X_3	0.100	*0.6494*	of fit = 0.8424
	X_2X_3	0.000	*1.0000*	
	X_1^2	-0.13	*0.5630*	
	X_2^2	-0.63	*0.0323*	
	X_3^2	0.92	*0.0081*	
Encapsulation efficiency (Y_3)	Intercept	25.37		F = 72.29,
	X_1	1.08	*< 0.0001*	R^2 = 0.9924,
	X_2	0.72	*< 0.0001*	Model P-value
	X_3	0.15	*0.0442*	< 0.0001,

X_1X_2	0.19	*0.0569*	*P*-value of lack of fit = 0.5970
X_1X_3	0.21	*0.0453*	
X_2X_3	0.057	*0.4986*	
X_1^2	0.70	*0.0004*	
X_2^2	-0.047	*0.5858*	
X_3^2	-0.034	*0.6900*	

S4 Analysis of response surfaces

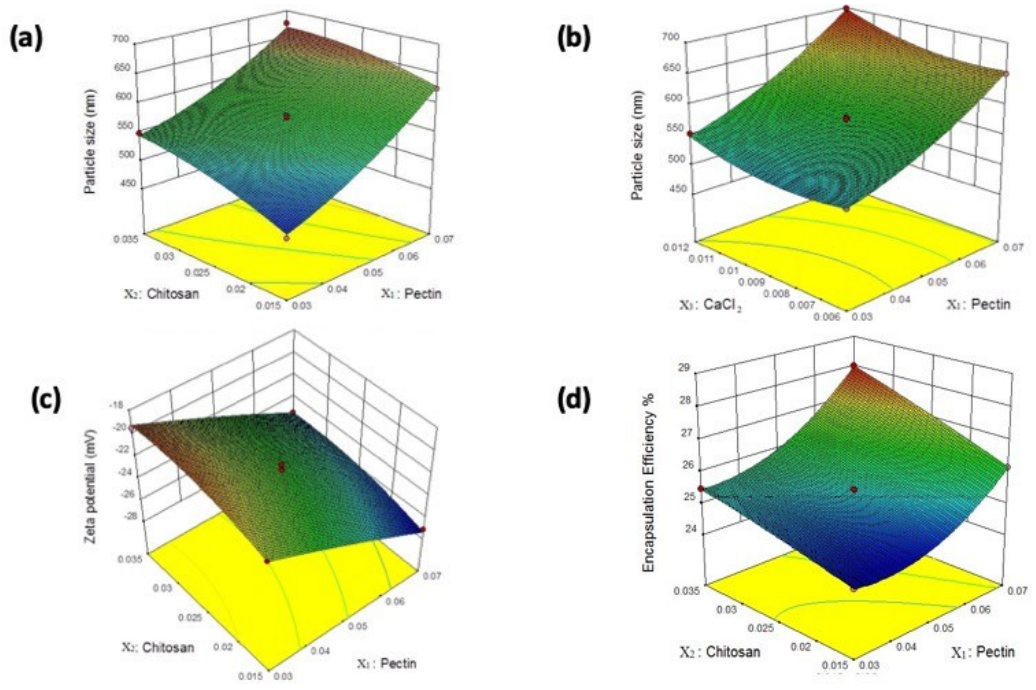

Fig. S2: Response surface showing (a) the effects of pectin (X_1) and chitosan (X_2) on the particle size at the mid-level of $CaCl_2$ (X_3), (b) the effects of pectin (X_1) and $CaCl_2$ (X_3) on the particle size at the mid-level of chitosan (X_2), (c) showing the effects of pectin (X_1) and chitosan (X_2) on ZP at the mid-level of $CaCl_2$ (X_3), and (d) showing the effects of Pectin (X_1) and chitosan (X_2) on EE% at the mid-level of $CaCl_2$ (X_3).

S5 Characterization of Pec/CS/JO NPs

- **TEM**

The size and shape of Pec/Cs and Pec/Cs/JO NPs were examined by TEM. The particles had a near spherical geometry within the polymeric chains. It can be observed that the mean diameter of Pec/CS NPs was about 55±3nm (Fig. S3[a] and [c]). After incorporation of JO (10 mg) in Pec/CS NPs (Fig. S3[b] and [d]), the diameter of the Pec/CS/JO NPs increased to approximately 150±4nm, indicating that the encapsulation of JO in Pec/CS network was successful. It is worth mentioning that the DLS was also used to determine the average size of the Pec/Cs and Pec/CS/JO NPs.

DLS measurements of Pec/CS NPs showed an average diameter of 504.8nm while Pec/CS/JO NPs had a size of 739.4 nm. The significant difference between the average sizes determined by both TEM and DLS might be linked to the physical form of the materials used. TEM measurements are performed on dry matter with restricted particle mobility while in DLS the measurements are carried out in liquid suspension. Thus in DLS sizes are directly related to the hydrodynamic diameter of the sample in the solvated state [16].

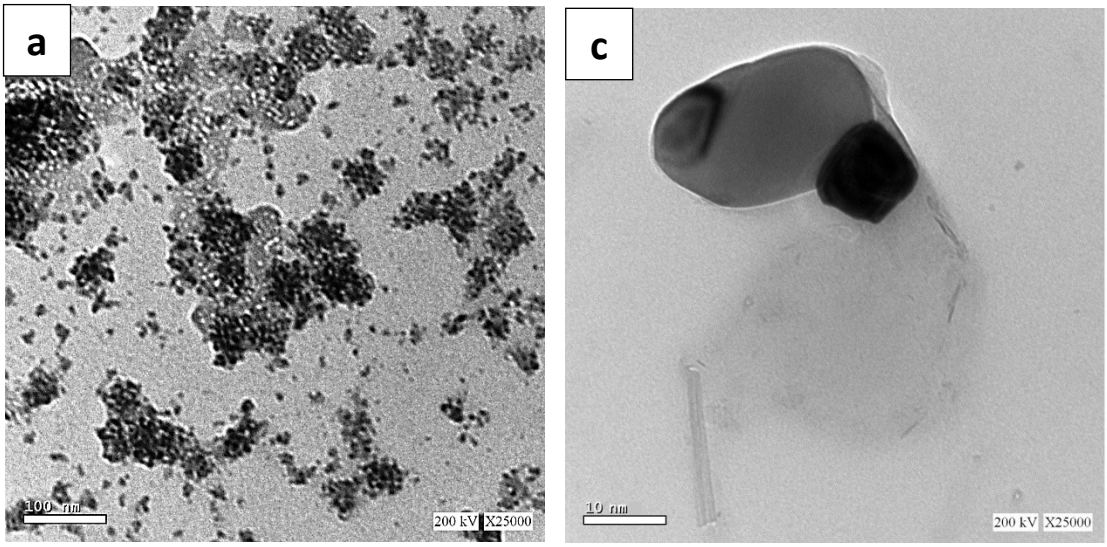

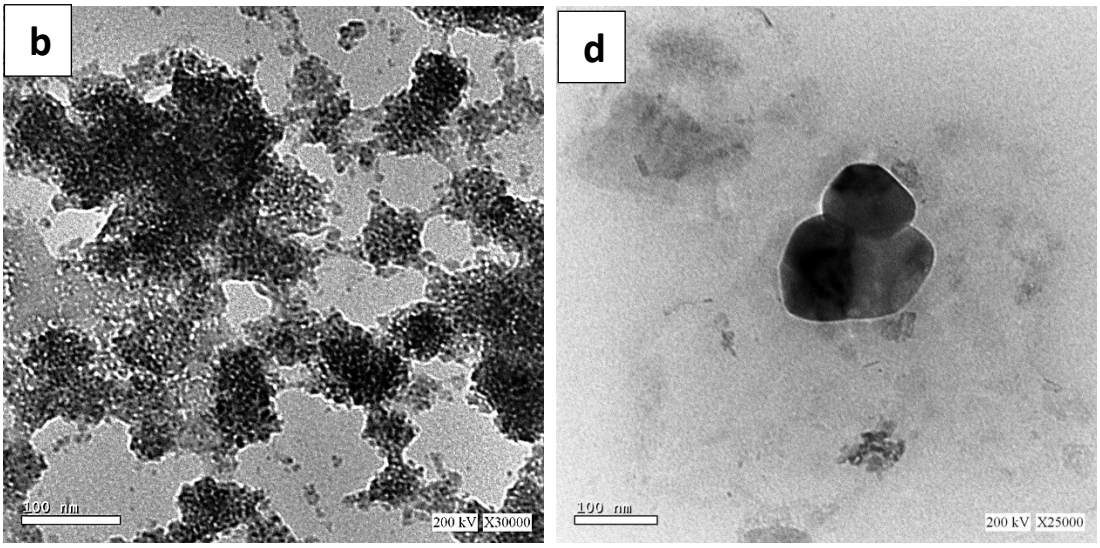

Fig. S3: TEM images of Pec/CS NPs (a, c), and Pec/CS/JO NPs (b, d).

- **FTIR Spectroscopy**

Fig. S4 shows the FTIR spectra of Pec powder, CS powder, Pec/CS NPs, JO and Pec/CS/JO NPs. The spectrum of Pec powder (Fig. S4[a]) showed a broad strong area of absorption at 3436 cm^{-1} represented by the stretching of O—H groups of carboxylic acid. The peak at 2943 cm^{-1} is related to C—H stretching vibration. Stronger bands occurring at approximately 1751 cm^{-1}, and at 1638 cm^{-1}, indicated the ester carbonyl (C=O) group and carboxylate ion stretching band (COO^{-}), respectively. The absorption patterns between 1300 and 800 cm^{-1} are referred to as the fingerprint region that is unique to pectin. CS powder showed a broad absorption peak between 3398 and 3170 cm^{-1} (Fig. S4[b]) attributed to a combination of stretching modes of O-H and N-H bonds in CS and to hydrogen bonds among polysaccharide chains. The main peaks recognized for the CS are related to C=O stretching amide I at 1653 cm^{-1} and to amide II at 1558 cm^{-11}.

The introduction of CS solution with Ca^{2+} as co-acervation/cross-linking agents resulted in the formation of Pec/CS NPs and this led to the change of some peaks relative to the carboxylic groups of Pec and amide groups of CS. As shown in the spectra of Pec/CS NPs (Fig. S4[c]), the two characteristic peaks of CS disappeared giving only one peak at 1530 cm^{-1}. A peak at 1417.5 cm^{-1} was identified and attributed to C-OH stretching of the carboxylic group [1]. In addition, the ester carbonyl (C=O) group was shifted from 1751 to 1743 cm^{-1}, and a strong carboxylate ion stretching band (COO^{-}) with increasing amplitude appeared at 1622 cm^{-1}, implying the complex formation.

As shown in (Fig. S4[d]), the main characteristic absorption peaks of pure JO are at 1739 cm^{-1} for (C=O stretching of ester), 1681 cm^{-1} for (C=O stretching) and (COO^{-} ion stretching) is indicated by 1624 cm^{-1} and 1575 to 1513 cm^{-1}. The appearance of these peaks in the spectra of Pec/CS/JO NPs (Fig. S4[e])

demonstrated the entrapment of JO. It can also be observed that there was no new absorption peak or shifting in the spectra of Pec/CS/JO NPs, indicating minor or no interaction between functional group of JO and polymers. Moreover, the fingerprint regions of the Pec/CS/JO NPs were similar to Pec/CS complex.

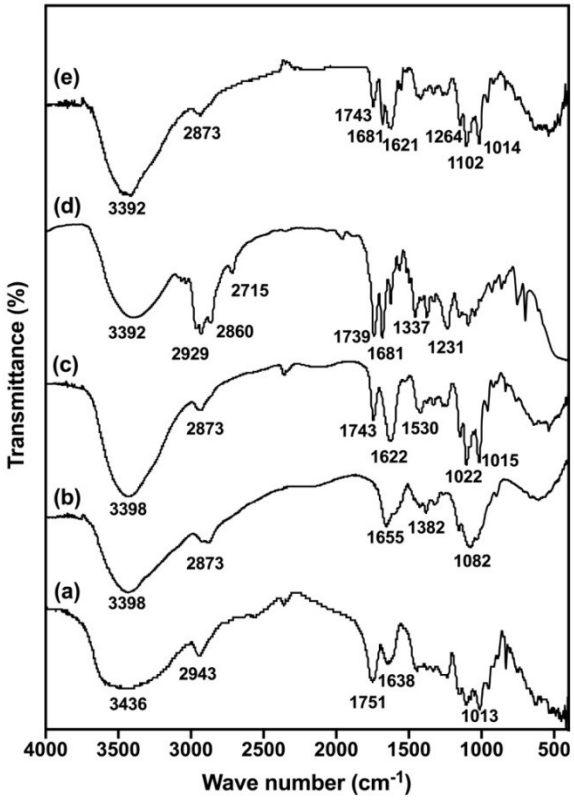

Fig. S4: FTIR spectra of: [a] Pec powder, [b] Pec NPs, [c] Pec/CS NPs, [d] Pure JO and [e] Pec/CS/JO NPs

- **XRD**

Crystallographic properties of Pec powder, Pec/CS NPs and Pec/CS/JO NPs were evaluated using X-ray diffraction (XRD). As shown in (Fig. S6[a]), XRD pattern of Pec powder displayed two characteristic peaks, the first peak at 2θ of 10^{o} and the second peak at 20^{o} indicating a high degree of crystallinity. The XRD patterns of Pec/CS NPs (Fig. S6[b]) and Pec/CS/JO NPs (Fig. S6[c]) showed a broad typical hump of amorphous material with an absence of the characteristic crystalline Pec peaks, indicating that Pec was changed to a noncrystalline form by the preparation process.

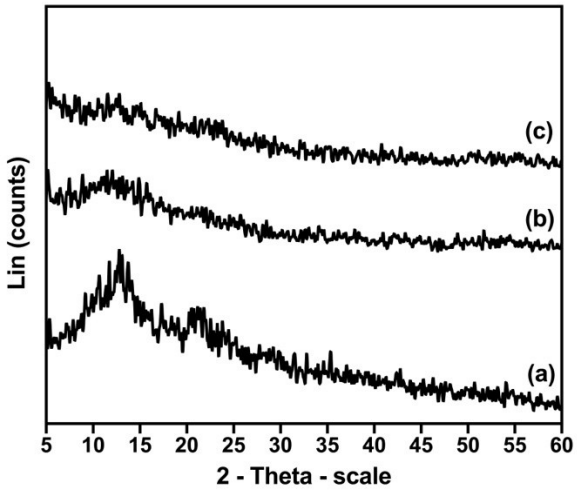

Fig. S5: XRD pattern of [a] Pec powder, [b] Pec/CS NPs and [c] Pec/CS/JO NPs

- **EDX**

SEM/EDX analysis was done for Pec NPs, Pec/Cs NPs and Pec/Cs/JO NPs to confirm the formation of the desired nanoparticulate system. Results indicated the presence of five main components (carbon, oxygen, nitrogen, Calcium and chloride) (**Fig. S7**). Noticeably, nitrogen was only present is Pec/Cs and Pec/Cs/JO NPs which indicates the incorporation of CS polymer in the NPs. In addition, carbon content was increased in Pec/CS/JO NPs which confirm the encapsulation of JO within the polymer network.

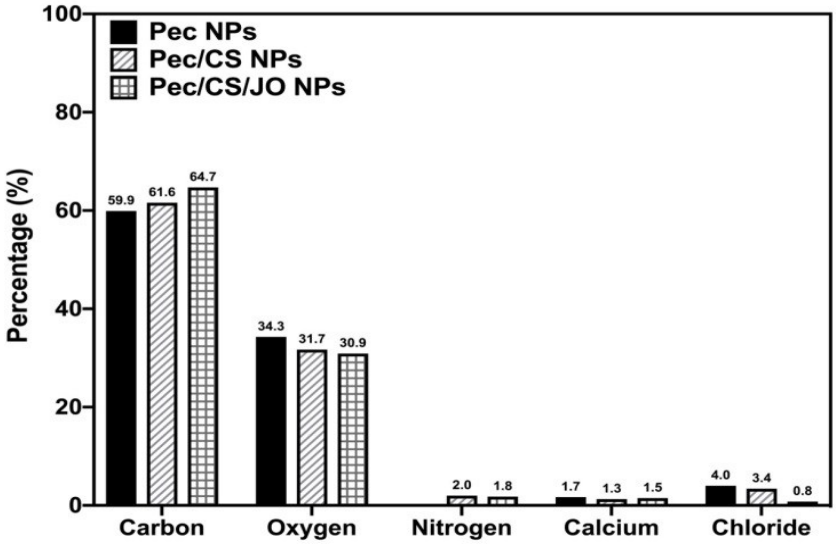

Fig. S6: SEM/EDX elemental analysis of pectin NPs, Pec/CS NPs and Pec/CS/JO NPs

S6 Swelling index

Swelling index study was performed on Pec/CS and Pec/CS/JO NPs that were weighed initially at ±10.0mg and placed in distilled water at (25 °C) for 24 hrs. Sample surface water was then removed and wet NPs mass was weighed. Swelling index was determined based on equation (3) [17].

$$SI\ (\%) = \frac{W_s - W_d}{W_d} \times 100 \qquad (3)$$

For: Ws: Swelling NPs Weight, W_d: Dried NPs Weight, SI: Swelling Index

Swelling index was studied to get more insights on the impact of the oil encapsulation on the inotropic gelation process. Swelling of Pec/CS/JO NPs, is mainly influenced by ionic interactions between Pec chains, CS chains and $CaCl_2$ during the formation of the nanoparticles [11]. An increase in cross-linking density is reported to induce a decrease in swelling [11]. The SI for Pec/CS NPs and Pec/CS/JO NPs were found to be 2.81± 0.13, and 8.83± 0.24%, respectively. Such difference indicates that the presence of JO in Pec/CS/JO NPs system influenced the crosslinking density during the fabrication process.

S7 *In-vitro* release study kinetics

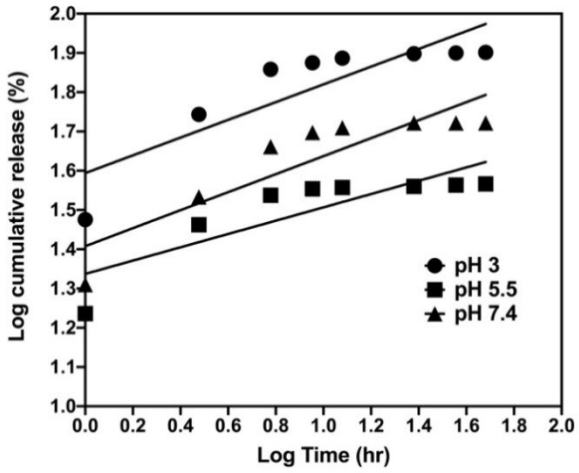

Fig. S7: Korsmeyer-Peppas kinetic plots of JO release from Pec/CS NPs at pH 3, 5.5, and 7.4

Table S5: Kinetics data of JO release from Pec/CS/JO NPs at different pH values

	Zero order		First order		Hixson Crowell		Higuchi		Korsmeyer Peppas		
	K	**R^2**	**K**	**R^2**	**K**	**R^2**	**K**	**R^2**	**K**	**R^2**	**n**
pH (3)	0.63	0.38	0.01	0.32	0.01	0.34	6.33	0.56	39.26	0.72	0.22
pH (5.5)	0.22	0.33	0.00	0.28	0.00	0.30	2.31	0.50	21.74	0.71	0.16
pH (7.4)	0.47	0.4	0.01	0.33	0.01	0.35	4.66	0.58	23.28	0.76	0.26

References

1 A. Rampino, M. Borgogna, B. Bellich, P. Blasi, F. Virgilio and A. Cesàro, *Eur. J. Pharm. Sci.*, 2016, **84**, 37–45.

2 S. O. Syed Mohamad Al-Azi, Y. T. F. Tan and T. W. Wong, *React. Funct. Polym.*, 2014, **84**, 45–52.

3 P. Ahlin Grabnar and J. Kristl, *Pharmazie*, 2010, **65**, 851–852.

4 H. Jonassen, A. Treves, A. L. Kjøniksen, G. Smistad and M. Hiorth, *Biomacromolecules*, 2013, **14**, 3523–3531.

5 S. Pistone, F. M. Goycoolea, A. Young, G. Smistad and M. Hiorth, *Eur. J. Pharm. Sci.*, 2017, **96**, 381–389.

6 G. C. Derringer, *Qual. Prog.*, 1994, **27**, 51–58.

7 I. Guideline, *Fed. Regist*.

8 I. Guideline, *Q2*.

9 *International Conference on Harmonization (ICH), Q2B, Validation of Analytical Procedures: Definitions and Terminology, Vol.60, US FDA Federal Register, 1995*, .

10 C. Deka, D. Deka, M. M. Bora, D. K. Jha and D. K. Kakati, *J. Drug Deliv. Sci. Technol.*, 2016, **35**, 314–322.

11 A. Shetta, J. Kegere and W. Mamdouh, *Int. J. Biol. Macromol.*, 2019, **126**, 731–742.

12 P. L. Ritger and N. A. Peppas, *J. Control. Release*, 1987, **5**, 37–42.

13 R. W. Korsmeyer, R. Gurny, E. Doelker, P. Buri and N. A. Peppas, *Int. J. Pharm.*, 1983, **15**, 25–35.

14 T. Higuchi, *J. Pharm. Sci.*, 1961, **50**, 874–875.

15 A. Esmaeili and A. Asgari, *Int. J. Biol. Macromol.*, 2015, **81**, 283–290.

16 L. Keawchaoon and R. Yoksan, *Colloids Surfaces B Biointerfaces*, 2011, **84**, 163–171.

17 A. Fahrurroji, D. Thendriani and H. Riza, *Int. J. Pharm. Pharm. Sci.*, 2017, **9**, 98.